Science of the Total Environment 856 (2023) 159142

Contents lists available at ScienceDirect

Science of the Total Environment

journal homepage: www.elsevier.com/locate/scitotenv

# Iron-sulfur geochemistry and acidity retention in hydrologically active macropores of boreal acid sulfate soils: Effects of mitigation suspensions of fine-grained calcite and peat

Changxun Yu [a,*], Eva Högfors-Rönnholm [b], Pekka Stén [c], Sten Engblom [b], Mats E. Åström [a]

[a] Department of Biology and Environmental Science, Linnaeus University, 39231 Kalmar, Sweden
[b] Research and Development, Novia University of Applied Sciences, 65200 Vaasa, Finland
[c] Environmental Technology, Vaasa University of Applied Sciences, 65200 Vaasa, Finland

## HIGHLIGHTS

- The macropore surfaces in boreal acid sulfate soils are covered by Fe/S-rich layers.
- The Fe/S-rich layers were dominated by Fe oxyhydroxysulfates (schwertmannite and jarosite).
- Hydrolysis of jarosite on macropore surfaces acts as a long-term acidification source.
- Calcite (alone and in combination with peat) promoted pH increase and jarosite hydrolysis.
- Peat alone induced a (near-)complete transformation of jarosite to Fe hydroxides.

## GRAPHICAL ABSTRACT

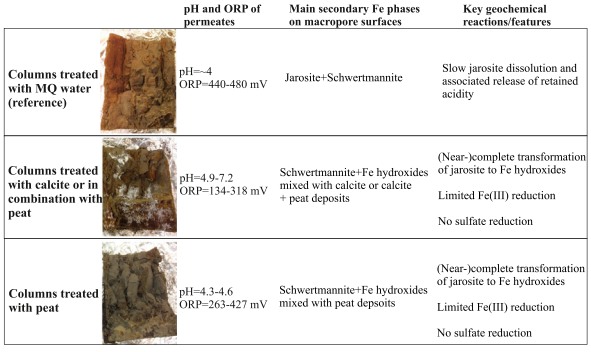


## ARTICLE INFO

Editor: Filip M.G. Tack

*Keywords:*
Iron and sulfur
Boreal zone
Metals
Remediation
Schwertmannite
Jarosite

## ABSTRACT

Acid sulfate soils discharge large amounts of sulfuric acid along with toxic metals, deteriorating water quality and ecosystem health of recipient waterbodies. There is thus an urgent need to develop cost-effective and sustainable measures to mitigate the negative effects of these soils. In this study, we flushed aseptically-prepared MQ water (reference) or mitigation suspensions containing calcite, peat or a combination of both through 15-cm-thick soil cores from an acid sulfate soil field in western Finland, and investigated the geochemistry of Fe and S on the surfaces of macropores and in the solid columnar blocks (interiors) of the soil columns. The macropore surfaces of all soil columns were strongly enriched in total and HCl-extractable Fe and S relative to the interiors, owing to the existence of abundant Fe oxyhydroxysulfates (schwertmannite and partly jarosite) as yellow-to-brownish surface-coatings. The dissolution/hydrolysis of Fe oxyhydroxysulfates (predominantly jarosite) on the macropore surfaces of the reference columns, although being constantly flushed, effectively buffered the permeates at pH close to 4. These results suggest that Fe oxyhydroxysulfates accumulated on the macropore surfaces of boreal acid sulfate soils can act as long-lasting acidification sources. The treatments with mitigation suspensions led to a (near-)complete conversion of jarosite to Fe hydroxides, causing a substantial loss of S. In contrast, we did not observe any recognizable evidence indicating transformation of schwertmannite. However, sulfate sorbed by this mineral might be partially lost through anion-exchange processes during the treatments with calcite. No Fe sulfides were found in the peat-treated columns. Since Fe sulfides can support renewed acidification events, the moderate mineralogical changes induced by peat are desirable. In addition, peat materials can act as toxic-metal scavengers. Thus, the peat materials used here, which is relatively cheap in the boreal zone, is ideal for remediating boreal acid sulfate soils and other similar jarosite-bearing soils.

* Corresponding author.
*E-mail address:* changxun.yu@lnu.se (C. Yu).

http://dx.doi.org/10.1016/j.scitotenv.2022.159142
Received 19 July 2022; Received in revised form 22 September 2022; Accepted 27 September 2022
Available online 30 September 2022

## 1. Introduction

Acid sulfate soils are formed when fine-grained sulfide-rich sediments (deposited on sea and lake bottoms) are brought into contact with atmospheric $O_2$, due to natural phenomena (e.g., land uplift and droughts) or human activities (e.g., drainage and excavations) (Ljung et al., 2009; Boman et al., 2010; Karimian et al., 2018). As the "nastiest soils on earth" (Dent and Pons, 1995; Ljung et al., 2009), the acid sulfate soils can discharge large quantities of acid and high levels of potentially toxic metals (e.g., Al, Cd, Ni, Cu etc.), imposing deleterious impacts on water quality and ecosystem health in receipt waterbodies (Hudd and Kjellman, 2002; Fältmarsch et al., 2008; Wong et al., 2010). Globally, acid sulfate soils occur widely on many low-lying coastal plains/lowlands, occupying a total area of at least 14–24 million ha (Andriesse and Van Mensvoort, 2006). In Europe, the soils are mainly found along the Baltic coasts of Finland (160,000–300,000 ha) and Sweden (50,000–140,000 ha), and were frequently reported to cause substantial ecological deteriorations, such as massive fish kills (Åström and Spiro, 2000; Yli-Halla et al., 2006; Fältmarsch et al., 2008; Nystrand et al., 2016).

During the formation of acid sulfate soils, the oxidation of sulfide minerals (mainly pyrite and metastable iron sulfides) produces a large amount of acidity and high levels of Fe and sulfate, leading to the precipitation of a range of poorly soluble Fe(III) oxyhydroxides (e.g., ferrihydrite) and oxyhydroxysulfates (e.g., schwertmannite and jarosite) within the soils and associated waterbodies (Bigham and Nordstrom, 2000; Collins et al., 2010; Fitzpatrick et al., 2017; Karimian et al., 2018). In acid sulfate soil landscapes with slightly higher pH (pH = 4.5–5), sulfate can be additionally retained as Al(III) oxyhydroxysulfates (e.g., basaluminite) (Bigham and Nordstrom, 2000; Jones et al., 2011). These secondary Fe(III) and Al (III) minerals are metastable, and thus can progressively transform into thermodynamically more stable forms (Bigham and Nordstrom, 2000; Burton et al., 2008; Vithana et al., 2015; Kölbl et al., 2021), during which trace metal(loid)s retained by the metastable minerals (via surface sorption or structural substitution) might be partially released or become more labile (Burton and Johnston, 2012; Karimian et al., 2017; Schoepfer and Burton, 2021). In addition, the transformation of Fe(III)/Al(III) oxyhydroxysulfates to Fe(III)/Al(III) hydroxides liberates substantial amounts of additional acidity, thus sustaining a high and long-lasting level of acidity in well-oxidized acid sulfate soils (Vithana et al., 2013; Karimian et al., 2018). Under certain conditions (e.g., rainy seasons), these secondary Fe(III) and sulfate minerals in acid sulfate soils (in particular those retained within deep soil layers) may undergo partial reduction driven by anaerobic oxidation of organic matter (Karimian et al., 2018), resulting in a marked increase in alkalinity and pH-induced immobilization of metals in these soil layers. Hence, secondary Fe–S minerals in acid sulfate soils are highly reactive and involved in periodically alternating redox-driven processes, which undoubtedly exerts an important control on acid dynamic and metal mobility in the soils.

The development of acid sulfate soils (e.g., drainage-induced soil shrinkage) also creates massive irreversible macropores (consisting of interconnected cracks, fissures, tubular macropores and other voids) with distinct hydraulic and physical properties (Dent, 1986; Johnston et al., 2009b). The interconnected macropore networks favor the gas exchange between the soil and atmosphere, resulting in the oxidation of sulfide minerals and release of associated metals in deep unoxidized or partially-oxidized soil layers (Johnston et al., 2009b). Furthermore, macropores efficiently promote the movements and transport of reactive solutes through percolating waters and capillary moistures within soil profiles (Jarvis, 2007; Beven and Germann, 2013). In addition, the surfaces of macropores in the acidic layer particularly within boreal AS soils are covered by abundant reddish-to-brownish fine-grained secondary Fe precipitates (Högfors-Rönnholm et al., 2022), leading to an overall limited leaching of Fe (in contrast to many other metals) in typical boreal acid sulfate soils (Åström, 1998; Österholm and Åström, 2002). However, the mineralogical and chemical composition of these Fe precipitates in macropores are poorly characterized in boreal acid sulfate soils, significantly hampering our understanding of how these precipitates and associated biogeochemical processes regulate the migration and export of trace metal(loid)s in the soils.

In the past decades, many laboratory- and field-based experiments have been conducted to test and develop different methods/techniques for minimizing the leaching of acid and metals from acid sulfate soils in both boreal and (sub-)tropical zones (Bärlund et al., 2005; Österholm et al., 2005; Johnston et al., 2009a; Creeper et al., 2015a; Dang et al., 2016; Kölbl et al., 2022). Controlled drainage and subsurface irrigation techniques have been tested and implemented in different acid sulfate soil experimental fields in Finland, but overall have had limited impact on acid generation and metal leaching (Bärlund et al., 2005; Österholm et al., 2005; Åström et al., 2007; Österholm et al., 2015). It has been shown that seawater or freshwater inundation could efficiently stimulate proton-consuming reductive processes (e.g., hydrolysis or reduction of secondary Fe oxyhydroxysulfates) in acid sulfate soils (Johnston et al., 2009a; Creeper et al., 2015a; Creeper et al., 2015b), provided that they contain sufficient easily mineralizable organic matter (Muhrizal et al., 2006; Kölbl et al., 2017; Kölbl et al., 2018). This method is, however, not applicable to acid sulfate soils that are being used as farmlands or located far away from seashore and freshwater bodies. In comparison to direct neutralization of acid sulfate soils with strong alkaline materials (e.g., lime) which are expensive and not readily available, amendments with various forms of naturally occurring organic materials (e.g., peat, plant/crop residues, biochars, compost, manure) are much more cost-effective (Dang et al., 2015; Michael et al., 2015), and therefore have been emerging as promising amelioration strategies for various acid sulfate soils (Muhrizal et al., 2007; Michael et al., 2015; Jayalath et al., 2021; Kölbl et al., 2022). A lab-experiment with repacked acid sulfate soil cores (finely-ground and approximately 2 cm thick) has shown that mixing organic materials into the soils before repacking is more effective in reducing acid production than placing them as a layer on top of the cores (Yuan et al., 2016). Given the facts that acidic layers of natural acid sulfate soil fields are much thicker and more compact than those used in the experiment (and can be additionally covered by an 20–40 cm thick cultivated layer), organic amendments to the top layers of natural acid sulfate soils (via physical mixing or adding as a layer) may be ineffective or provide limited effect on the deeper acidic layers where most of acidity is produced/stored. Therefore, there is an urgent need to find a practical and effective way to apply these methods in "real" field scales. Recently, some researchers carried out several column experiments by slowly injecting suspensions of fine-grained peat in combination with strong alkalis into hydrologically active macropores in intact acid sulfate soil cores (15 cm thick), and got similar results as other experiments for which acid sulfate soil and organic materials were physically mixed (Wu et al., 2013; Högfors-Rönnholm et al., 2022). These suspensions can be easily applied to natural acid sulfate soils through subsurface irrigation techniques that have been well-tested and implemented in many acid sulfate soil fields, in particular in Finland. However, these previous column studies mainly focused on how the chemistry of the permeates and bacterial community responded to the treatments with different suspensions. The impacts of these suspensions on the mineralogy and chemical status of Fe and S that are accumulated on the surface of the hydrologically active macropores are still largely unknown.

Högfors-Rönnholm et al. (2022) carried out a column experiment during which different mitigation suspensions (with peat, Ca-carbonate or a combination of both) were slowly flushed through intact soil columns sampled from an acid sulfate soil experimental field in Finland (Risöfladan). By using soil columns treated solely with MQ as references, they investigated changes in the treated columns in terms of (i) the physicochemical properties of permeates; and (ii) microbial communities and metal distributions within solid columnar blocks (which they call "inner-core") and on the surface of macropores. During the column experiment, Fe–S geochemistry and linked geochemical processes on the surface of macropores should have been strongly altered/affected by the mitigation suspensions but are yet to be investigated. In a follow-up study presented here, we (i) explored how and in which phases Fe and S are accumulated on the surface of

macropores in the reference soil columns that can be considered to represent a typical acid sulfate soil in the boreal zone; and (ii) investigated how the mineralogy and chemical status of secondary Fe and S phases (in particular those sitting on macropores) have responded to different mitigation suspensions, thereby influencing acid production as well as the leaching and environmental fate of metals.

## 2. Materials and methods

### 2.1. Soil column experiments

Six parallel column experiments were carried out in duplicate using 15 cm thick soil cores collected from the oxidized soil layers (between 70 and 85 cm below the ground surface) of the Risöfladan experimental acid sulfate soil field in Vaasa, Western Finland (63°02′50″ N, 21°42′42″ E). Details of the area as well as the soil physicochemical properties and parameters of the experimental field have been reported previously (Åström et al., 2007; Boman et al., 2010; Wu et al., 2013; Högfors-Rönnholm et al., 2018). Briefly, the sampled soil cores (sealed in rubber membranes) were packed into columns and flushed with either aseptically prepared MQ (reference test, hereafter referred to as "R") or mitigation suspensions using a well-tested experimental apparatus, which could effectively avoid bypass flow and thus, allowing the MQ or mitigation suspensions to infiltrate through the network of hydrologically active macropores at controlled flow rates (50 or 100 mL/h). The mitigation suspensions included: (i) "$C_{2.5}$", an aqueous suspension with fine-grained calcium carbonate with a median particle diameter of 2.5 μm; (ii) "$C_{0.3}$", an aqueous suspension of 37 % ultrafine-grained $CaCO_3$ with a median particle diameter of 0.3 μm that includes the dispersing agent Alcoguard® H 5941; (iii) "P", an aqueous suspension with a fine-grained peat of biodegradation level H1 with a median particle diameter of 20 μm and a typical organic content of 95–98 %; (iv) "$C_{2.5}$P", referring to a combined treatment with "$C_{2.5}$" followed by "P"; and (v) "$C_{0.3}$P", referring to a combined treatment with "$C_{0.3}$" followed by "P". For iv and v, the suspensions were applied successively, such that calcite was introduced first and after that peat. After being flushing with the MQ or mitigation suspensions for 3–4 weeks, the soil cores (enclosed in the rubber membranes) were removed from the column apparatus, wrapped in aluminum foil, sealed tightly in plastic bags, and incubated for 4 weeks at 10 °C in the dark. The incubation attempted to provide additional time for the treatments to yield measurable impacts on relatively slow processes, such as solute diffusion, mineral transformations, and microbially-mediated reactions. More detailed information on the sampling of the soil cores and procedures of the column experiments (including preparation of the mitigation suspensions) are given in a parallel paper (Högfors-Rönnholm et al., 2022).

The pH of the permeates from the R and P columns remained around 4 during the experiment. In contrast, the pH of the permeates from the $C_{2.5}$ and $C_{0.3}$ columns increased from approximately 4 to 7 and for the columns $C_{2.5}$P and $C_{0.3}$P from approximately 4 to 6. More details are given in the parallel paper (Högfors-Rönnholm et al., 2022).

### 2.2. Samples

After the experiment, the soil columns were opened and split into smaller pieces by hand. Composite samples from macropore surface and from within solid columnar blocks (hereafter "interior") were obtained for each column, by scraping all exposed surfaces and underlying clayish parts, respectively. The collected samples were frozen, and then dried in a glove box ($O_2$ < 0.5 ppm) before being pulverized into powders.

The samples were listed in Table 1 and named as follows, from left to right: Uppercase Letter (R for reference columns, C for carbonate-treated columns, P for peat-treated columns), after C a subscript number with a decimal (grain size of the carbonate), number (1 or 2 referring to duplicate columns), subscript "surf" or "int" (referring to the macropore surface and interior, respectively) and subscript number (identifying the number of subsamples where such were taken). An uppercase P in the middle of the name means peat treatment followed after carbonate treatment.

**Table 1**
List of samples (and performed analyses) obtained from each soil column of this study.

| Column | Sampling location | Sample ID | Performed analyses |
|---|---|---|---|
| R1[a] | Macropore surface | R-$1_{surf-1}$ | 1 M KCl, 1 M HCl, 4 M HCl, "near-total" |
| | | R-$1_{surf-2}$ | 1 M KCl, 1 M HCl, 4 M HCl, "near-total" |
| | | R-$1_{surf-3}$ | HaHc, "near-total", Fe XAS |
| | Interiors | R-$1_{int-1}$ | 1 M KCl, 1 M HCl, 4 M HCl, "near-total" |
| R2[a] | Macropore surface | R-$2_{surf-1}$ | 1 M KCl, 1 M HCl, 4 M HCl, "near-total" |
| | | R-$2_{surf-2}$ | 1 M KCl, 1 M HCl, 4 M HCl, "near-total", Fe XAS |
| | | R-$2_{surf-3}$ | HaHc, "near-total", Fe XAS |
| | Interiors | R-$2_{int-1}$ | 1 M KCl, 1 M HCl, 4 M HCl, "near-total" |
| $C_{2.5}$-1[b] | Macropore surface | $C_{2.5}$-$1_{surf}$ | 1 M KCl, 1 M HCl, 4 M HCl, "near-total", Fe XAS |
| | Interiors | $C_{2.5}$-$1_{int}$ | 1 M KCl, 1 M HCl, 4 M HCl, "near-total", Fe XAS |
| $C_{2.5}$-2[b] | Macropore surface | $C_{2.5}$-$2_{surf}$ | 1 M KCl, 1 M HCl, 4 M HCl, "near-total", Fe XAS |
| | Interiors | $C_{2.5}$-$2_{int}$ | 1 M KCl, 1 M HCl, 4 M HCl, "near-total", Fe XAS |
| $C_{0.3}$-1[c] | Macropore surface | $C_{0.3}$-$1_{surf}$ | 1 M KCl, 1 M HCl, 4 M HCl, "near-total", Fe XAS |
| | Interiors | $C_{0.3}$-$1_{int}$ | 1 M KCl, 1 M HCl, 4 M HCl, "near-total" |
| $C_{0.3}$-2[c] | Macropore surface | $C_{0.3}$-$2_{surf}$ | 1 M KCl, 1 M HCl, 4 M HCl, "near-total", Fe XAS |
| | Interiors | $C_{0.3}$-$2_{int}$ | 1 M KCl, 1 M HCl, 4 M HCl, "near-total" |
| P1[d] | Macropore surface | P-$1_{surf-1}$ | 1 M KCl, 1 M HCl, 4 M HCl, "near-total" |
| | | P-$1_{surf-2}$ | HaHc, "near-total", Fe XAS |
| | | P-$1_{surf-3}$ | HaHc, "near-total", Fe XAS |
| | Interiors | P-$1_{int-1}$ | 1 M KCl, 1 M HCl, 4 M HCl, "near-total" |
| | | P-$1_{int-2}$ | HaHc, "near-total", Fe XAS |
| | | P-$1_{int-3}$ | HaHc, "near-total", Fe XAS |
| P2[d] | Macropore surface | P-$2_{surf-1}$ | 1 M KCl, 1 M HCl, 4 M HCl, "near-total" |
| | | P-$2_{surf-2}$ | HaHc, "near-total", Fe XAS |
| | | P-$2_{surf-3}$ | HaHc, "near-total", Fe XAS |
| | Interiors | P-$2_{int-1}$ | 1 M KCl, 1 M HCl, 4 M HCl, "near-total" |
| | | P-$2_{int-2}$ | HaHc, "near-total", Fe XAS |
| | | P-$2_{int-3}$ | HaHc, "near-total", Fe XAS |
| $C_{2.5}$P-1[e] | Macropore surface | $C_{2.5}$P-$1_{surf}$ | 1 M KCl, 1 M HCl, 4 M HCl, "near-total", Fe XAS |
| | Interiors | $C_{2.5}$P-$1_{int}$ | 1 M KCl, 1 M HCl, 4 M HCl, "near-total", Fe XAS |
| $C_{2.5}$P-2[e] | Macropore surface | $C_{2.5}$P-$2_{surf}$ | 1 M KCl, 1 M HCl, 4 M HCl, "near-total", Fe XAS |
| | Interiors | $C_{2.5}$P-$2_{int}$ | 1 M KCl, 1 M HCl, 4 M HCl, "near-total", Fe XAS |
| $C_{0.3}$P-1[f] | Macropore surface | $C_{0.3}$P-$1_{surf}$ | 1 M KCl, 1 M HCl, 4 M HCl, "near-total", Fe XAS |
| | Interiors | $C_{0.3}$P-$1_{int}$ | 1 M KCl, 1 M HCl, 4 M HCl, "near-total" |
| $C_{0.3}$P-2[f] | Macropore surface | $C_{0.3}$P-$2_{surf}$ | 1 M KCl, 1 M HCl, 4 M HCl, "near-total" |
| | Interiors | $C_{0.3}$P-$2_{int}$ | 1 M KCl, 1 M HCl, 4 M HCl, "near-total" |

[a] Duplicate reference soil columns treated with MQ.
[b] Duplicate soil columns treated with "$C_{2.5}$", that is, an aqueous suspension with fine-grained calcium carbonate with a median particle diameter of 2.5 μm.
[c] Duplicate soil columns treated with "$C_{0.3}$", that is, an aqueous suspension of 37 % ultrafine-grained $CaCO_3$ with a median particle diameter of 0.3 μm that includes the dispersing agent Alcoguard® H 5941.
[d] Duplicate soil columns treated with "P", that is, an aqueous suspension with a fine-grained peat of biodegradation level H1 with a median particle diameter of 20 μm and a typical organic content of 95–98 %.
[e] Duplicate soil columns treated with "$C_{2.5}$" followed by "P".
[f] Duplicate soil columns treated with "$C_{0.3}$" followed by "P".

### 2.3. Chemical analyses

Subsamples of all pulverized soil materials (including blind replicates) were randomized and subjected to a four-acid digestion. This included adding a sequence of three strong acids (hydrofluoric acid, followed by a mixture of nitric and perchloric acids) to 0.25 g of sample split, which was heated until incipient dryness was attained. Thereafter, sample was brought back into solution using aqua regia. This digestion method will dissolve also the most resistant minerals (Hall et al., 1996) and was commonly used for determining the "near-total" concentrations for most elements. In

addition, selected samples were subject to a hot HaHc leach, which involves reacting 0.75 g of sample split with 0.25 M $NH_2OH{\cdot}HCl$ in 0.25 M HCl at 60 °C for 2 h. This leach specifically attacks amorphous Fe-hydroxides and crystalline Mn-hydroxides as well as other acid-soluble minerals such as Al oxyhydroxides (Hall et al., 1996; Hall, 1998; Åström et al., 2012). The concentrations of Fe, S, Ca, K, Mg and Al in all resulting solutions were determined with an inductively coupled plasma mass spectrometer (ICP-MS/OES). Analyses of blanks were carried out to measure background, duplicates to monitor analytical precision, and a range of certificated reference materials (TILL-1 and -2, DNC-1a, and OREAS-72a, -101b, -904, -45d, -923, -621 and -522) to determine accuracy. According to the methods proposed by Gill (2014), the analytical precision was better than 6 %, while the accuracy was within ±12 %.

Selected soil materials were additionally subjected to three discrete leaches. Briefly, 0.4 g of sample splits were shaken with 16 mL 1 M KCl (4 h), 1 M HCl (4 h) and 4 M HCl (16 h) on an orbital shaker at 160 rpm. Thereafter, all suspensions were centrifuged at 8000 rpm for 15 min, and the supernatants were filtered through 0.45 μm syringe filters. The 1 M KCl extractants were acidified by ultrapure $HNO_3$. The concentrations of ferrous iron in the 1 M HCl extractants were immediately measured spectrophotometrically (the 1,10 phenanthroline method) with LCK 320 test kits using a Hach spectrophotometer (DR 1900). All extractants were analyzed for the concentrations of S, Ca, Fe, K, Mg and Al by ICP-OES. The 1 M KCl leach is expected to mainly recover soluble and exchangeable species, as well as soluble minerals (e.g., gypsum) and (very) minor amounts of poorly-crystalline Fe/Al hydroxides and/or oxyhydroxysulfates (e.g., schwertmannite and basaluminite). The 1 M HCl leach is expected to additionally recover "reactive" Fe from Fe sulfides (e.g., FeS), carbonates (e.g., siderite and calcite), poorly-crystalline Fe (hydr-)oxides and oxyhydroxysulfates (e.g., ferrihydrite schwertmannite) (Wallmann et al., 1993; Haese et al., 1997; Yu et al., 2021). As reported previously (Canfield, 1988; Claff et al., 2010), this leach may also lead to partial dissolutions of (hydr-)oxides/oxyhydroxysulfate with high degrees of crystallinity (e.g., hematite and jarosite) and some phyllosilicates (e.g., biotite and chlorite). The 4 M HCl leach can additionally extract a large proportion of poorly-crystalline Fe/Al hydroxides and Fe/Al oxyhydroxysulfates, along with some organically bound species (e.g., organic sulfur) (Ahern et al., 2004), plus more phyllosilicates that can be partially dissolved by 1 M HCl. The difference between the 4 M HCl extractable and 1 M KCl extractable fractions were used to define net acid soluble sulfur ($S_{NAS}$), iron ($Fe_{NAS}$) and aluminum ($Al_{NAS}$) retained largely in poorly insoluble Fe/Al hydroxides and Fe/Al oxyhydroxysulfates (Ahern et al., 2004; Vithana et al., 2013). In addition, 1 M HCl fraction and 4 M HCl fraction were defined as the differences between 1 M HCl and 1 M KCl extractable fractions, and between 4 M HCl and 1 M HCl extractable fractions, respectively, while residual fraction as the difference between "near-total" concentration and 4 M HCl extractable fraction.

### 2.4. Fe K-edge X-ray absorption spectroscopy

Iron K-edge X-ray absorption spectroscopy (XAS) was used to characterize solid-phase Fe speciation in selected soil materials. The samples (finely ground powders) were packed into Teflon holders and then sealed with two layers of Kapton tapes. The XAS data were collected in transmission mode at room temperature on several beamlines, including the HXMA beamline (06ID) of the Canadian Light Source, and the DUBBLE beamline (BM-26a) of the European Synchrotron Radiation Facility and the Balder beamline of the MAX IV laboratory. The XAS data collected at the Balder beamline were recorded from −200 to +570 eV relative to the Fe K-edge using a fly scan mode with a 0.5 eV step and an acquisition time of 0.5 s per step. To achieve satisfactory signal-to-noise ratios, 8–15 scans were recorded for each sample. At the other beamlines, XAS data (2–3 scans per sample) were recorded using different step sizes for the pre-edge (−200 to −30 eV, 5 eV per step), X-ray absorption near-edge structure (XANES) region (−30 to 50 eV, 0.25 eV per step) and Extended X-ray absorption fine structure (EXAFS) region (above 50 eV, 0.05 Å-1 per step), in-line with a Fe metal foil for internal energy calibration. No radiation-induced damage had occurred during the measurement, as individual XANES scans for each sample were identical.

To aid interpretations of the experimental XAS data, we compiled a total of 19 Fe reference spectra, representing a broad range of Fe oxidation states and coordination environments that could possibly occur in our samples, for details see Table S1 in the Supporting Information (SI). These reference spectra were either (i) collected during our previous experiments at the Balder beamline (Shahabi-Ghahfarokhi et al., 2022) and the beamline I811 of the MAX-lab (Yu et al., 2015; Yu et al., 2020); or (ii) provided directly by the corresponding author of Burton and Johnston (2012). All XAS spectra were analyzed using Demeter and SIXpack software packages, following standard procedures including energy calibration, averaging of multiple scans, background removal and normalization. EXAFS spectra were extracted from the normalized data using a cubic spline function. Principal component analysis (PCA) in combination with target transformation (TT) testing were applied to $K^3$-weighted EXAFS spectra, in order to identify suitable reference spectra for quantifying Fe speciation via a linear combination fitting (LCF) approach under the guidance of F-tests. The detailed information is given in SI-1.

## 3. Results

### 3.1. Iron

The Fe concentrations were several percentage units higher on the macropore surfaces than in the interiors (Figs. 1a, 2a), which was expected as the former were covered by visible brownish Fe precipitates. The residual fraction was significant and relatively constant across the samples, whereas the 1 M KCl-extractable fraction was very low in all the samples (Fig. 2a, Table S4). A major part of the Fe was released by the two HCl extractions. On the macropore surfaces of the peat-treated columns (P, $C_{2.5}P$, and $C_{0.3}P$) the 1 M HCl fraction was dominating, whereas for the other columns (not treated with peat) the 4 M HCl fraction was substantial however smaller than the 1 M HCl fraction (Fig. 2a). In the interiors, the 1 M HCl fraction dominated in the peat-treated columns whereas the 1 M and 4 M HCl fractions were equally abundant in the other columns (Fig. 2a). The 1 M HCl fraction was throughout dominated by Fe(III), with a nearly 100 % share (relative to Fe(II)) at high concentrations and down to nearly 80 % at low concentrations (Fig. 1b, Table S4). However, on the surfaces of macropores in two peat-treated columns ($P\text{-}1_{surf\text{-}1}$ and $C_{0.3}P\text{-}1_{surf}$), the 1 M HCl extractable Fe(II) was clearly elevated with concentrations up to nearly 1.2 % (Table S4), reflected as outliers in the plot of Fig. 1b.

There was a significant and relatively strong correlation between the proportions of Fe extracted by 1 M HCl or HaHc (targeting "reactive" and thus non-silicate bound Fe) and Fe bound in non-silicate phases as predicted by the LCF-EXAFS analysis (Fig. 1 c). This showed that there was a general agreement between the results provided by these two contrasting techniques. However, although many samples plotted along the 1:1 line, several others contained significantly higher proportions of 1 M HCl or HaHc extractable Fe than non-silicate bound Fe predicted by the LCF-EXAFS analysis (Fig. 1c). The discrepancy might reflect the inherent uncertainties in the LCF-EXAFS analysis, including (i) differences in the Fe bonding environment between pure reference materials and "actual" Fe phases in the soil samples, and (ii) similarity in the EXAFS spectra for some of the Fe references (Fig. S3). Furthermore, this discrepancy may also appear as a result of partial dissolution or structural alterations of some silicates under the acidic and reducing conditions during the 1 M HCl and HaHc extractions (Canfield, 1988; Favre et al., 2004; Wang et al., 2020). Given the uncertainties in the quantification of Fe speciation via the LCF-EXAFS analysis, only the robust features in the results of this analysis are highlighted, as shown in Table 2: On the macropore surfaces, (i) schwertmannite was generally the dominating secondary non-silicate Fe phase both in the reference and treated columns, although in some samples it was not detected; (ii) jarosite occurred in two out of three samples from the reference columns; (iii) 2-line ferrihydrite occurred in the peat-treated columns but

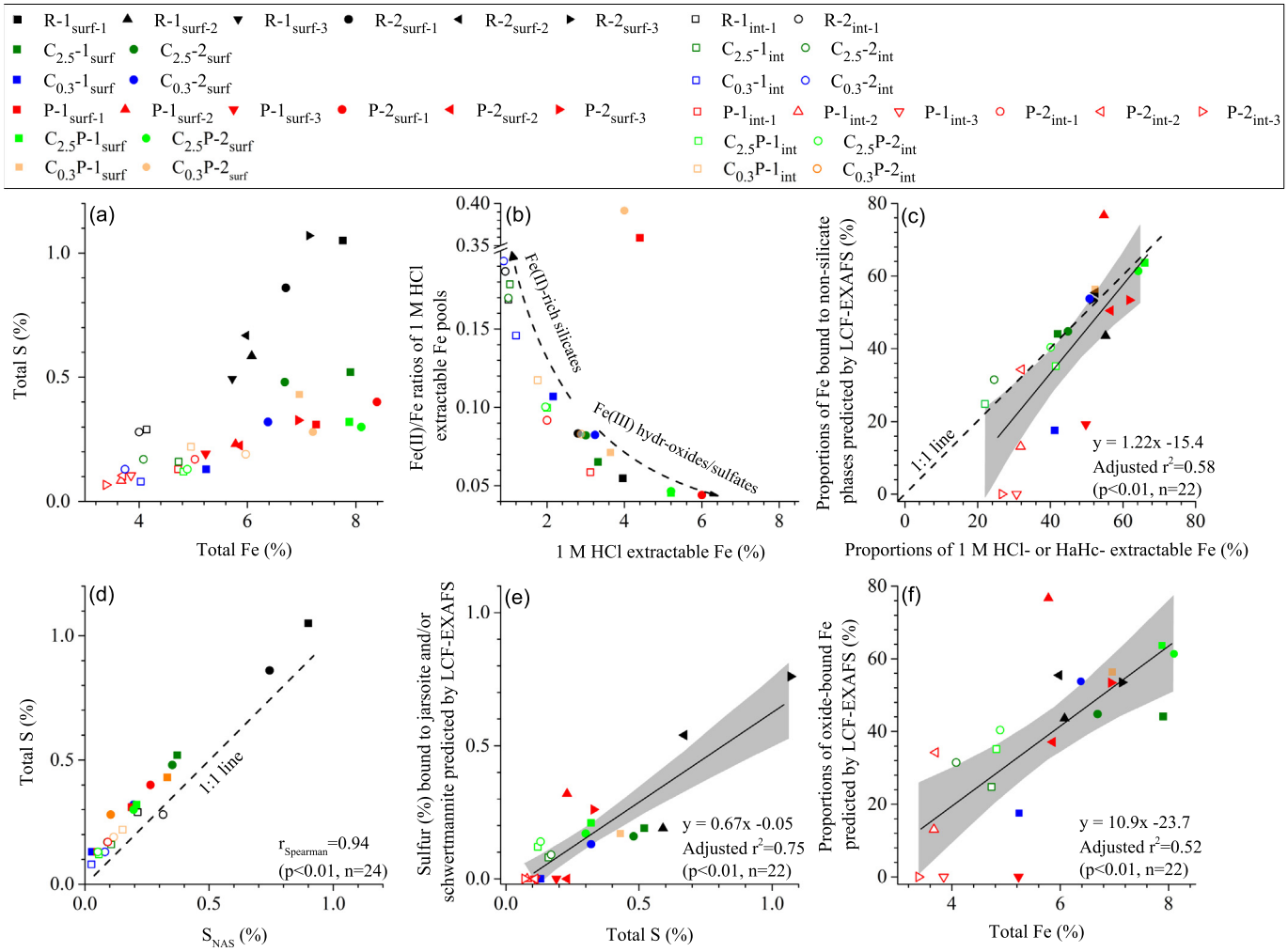


**Fig. 1.** Correlations between different Fe and S fractions (defined by chemical extractions or LCF-EXAFS analysis) on the macropore surfaces and in the interiors of the reference and treated soil columns. Detailed information on each of the samples (sampling columns/locations and performed analyses) are given in Table 1. The black solid lines are the best linear fits, while the shaded areas represent 95 % confidence interval.

only sporadically in the others; (iv) lepidocrocite was mostly found in the calcite-treated columns; and (v) substantial fractions of Fe in all the samples were associated with silicates, mainly as illite followed by hornblende/biotite. In the interiors, fewer samples were analyzed but suggested a dominance of silicates (with a roughly equal share of hornblende/biotite and illite), with additional frequent occurrence of schwertmannite. A detailed description of the XANES and EXAFS spectra as well as the LCF-EXAFS results are given in SI-2 and SI-3.

### 3.2. Sulfur

The S concentrations were consistently higher on the macropore surfaces than in the interiors, and much higher in the reference columns, both on the surfaces and in the interiors, than in the treated columns (Figs. 1a, 2b). The 1 M KCl-extractable S fraction was overall relatively minor but more abundant on the macropore surfaces than in the interiors with no clear difference among the treatments/reference (Fig. 2b, Table S5). This S fraction displayed no correlation with (i) the 1 M KCl-extractable fractions of Fe, Al and Ca (more details on these three metals are given below) (Fig. 3a-c); (ii) the $Al_{NAS}$ fraction (Fig. 3d); and (iii) the 4 M HCl Fe fraction (Fig. 3e), but was strongly correlated with 1 M HCl-extractable Fe(III) (and 1 M HCl-extractable Fe, data not shown) (Fig. 3f) . Also the residual S fraction was minor and thus, S was largely extractable with HCl (Fig. 2b). In the peat-treated columns (P, $C_{2.5}P$, and $C_{0.3}P$), the 1 M HCl fraction was dominating whereas for the other columns (not treated with peat) the 4 M HCl fraction was generally dominating (Fig. 2b). As a consequence of these extractability features, the total S concentrations were just slightly higher than, and strongly correlated with, $S_{NAS}$ (Fig. 1d) that was expected to host mainly oxyhydroxysulfate minerals. Since some of the samples with Fe EXAFS data were not analyzed for $S_{NAS}$, the LCF-EXAFS derived concentrations of schwertmannite + jarosite bound S were compared with the concentrations of total S (instead of $S_{NAS}$). There was an overall match between these two variables (Fig. 1e).

### 3.3. Magnesium, K, Al and Ca

The metals Mg, K, Al and Ca were dominated by the residual fraction (Tables S6-S9), which was not surprising as these metals were expected to be largely associated with silicates in acid sulfate soils (Åström and Björklund, 1997). The more easily extractable fractions are presented in Fig. 4. Key features were: (i) the 4 M HCl-fraction of K was clearly enriched in three macropore-surface samples, of which two occurred in the reference columns, in line with the detection of jarosite on the macropores of these columns; (ii) the 1 M KCl and 1 M HCl fractions of Ca were expectedly strongly enriched in the carbonate-treated columns ($C_{2.5}$ and $C_{0.3}$) in particular on the macropore surfaces, and also enriched but to a smaller extent in the columns treated with first carbonate and then peat ($C_{2.5}P$ and $C_{0.3}P$); and (iii) Mg and Al were relatively constant throughout the columns without any clear trends.

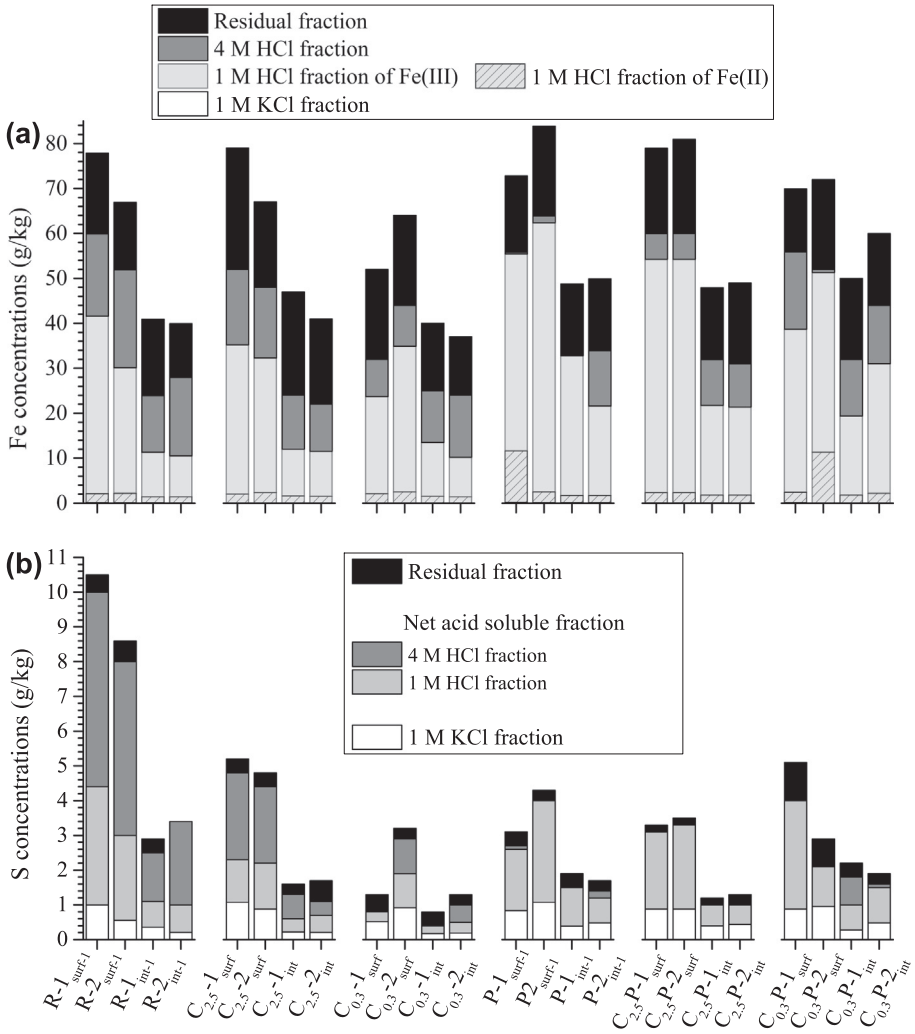


**Fig. 2.** Concentrations of different fractions of Fe and S on the macropore surfaces and in the interiors of reference and treated soil columns. Detailed information on each of the samples (sampling columns/locations and performed analyses) are given in Table 1. The residual, 4 M and 1 M HCl fractions were determined by difference: "near-total" concentration – 4 M HCl extractable concentration, 4 M HCl extractable concentration – 1 M HCl extractable concentration, and 1 M HCl extractable concentration – 1 M KCl extractable concentration, respectively.

## 4. Discussion

### *4.1. Major geochemical characteristics of the macropore surfaces*

The macropore surfaces of the reference columns were covered by abundant yellowish-to-brownish precipitates, which is a typical feature for acid sulfate soils in the boreal zone. These precipitates were still abundant and visible on the macropore surfaces of the treated columns but mixed with either white carbonate deposits or dark peat materials of varying thickness (Högfors-Rönnholm et al., 2022), suggesting that the mitigation suspensions have flowed through the macropore systems and thus been in close contact with the precipitates. The macropore surfaces were enriched in Fe and S, relative to the interiors, in both the reference and treated columns (Fig. 1a). This feature was also evident at the macro- and micro-scales as revealed by previous XRF analyses of the same columns (Högfors-Rönnholm et al., 2022). The XRF analyses also showed that the enrichment of Fe and S was mirrored by a parallel decrease in silicate-bound elements (Al, Si, and Mg), suggesting the formation of secondary Fe –S phases on the macropore surfaces. Indeed, our data also showed that the Fe and S pools on the macropore surfaces were dominated by the HCl-extractable fractions (Fig. 2), overall in line with the relatively high fractional amounts of oxide-bound Fe as well as oxyhydroxysulfate bound S as predicted by the LCF-EXAFS analysis (Fig. 1c,e,f and Table 2).

### *4.2. Accumulation of Fe and S on the macropore surfaces under natural conditions (reference columns): chemical forms, mechanisms, and acidity retention*

Jarosite and schwertmannite were the only minerals in the oxide pool on the macropore surfaces of the reference columns, as predicted by our LCF-EXAFS analysis (Table 2). This matches with: (i) the physicochemical data of the permeates from these columns (e.g., Eh-pH diagram) pointing to an equilibrium between these two phases in the system (Högfors-Rönnholm et al., 2022); and (ii) the feature that the macropore surfaces of the reference columns were enriched, relative to the treated columns, with 4 M HCl extractable K but not Mg and Al (Fig. 4) supporting that jarosite, which typically contains K and is expected to be largely dissolved by the 4 M HCl leach, occurred on these surfaces. Given the fact that the macropore surfaces in the oxidized soil horizon of the Risöfladan experimental field (where the soil columns were collected) are heavily covered by brownish precipitates and the reference columns were only flushed with MQ water, schwertmannite and jarosite were certainly formed in the field. The reduced/sub-oxic soil layers underlying the oxidized soil horizon

**Table 2**
Solid-phase speciation of Fe in selected soil materials collected from the macropore surfaces and interiors of different soil columns, quantified by linear combination fitting of $K^3$-weighted EXAFS spectra (k = 2–11.5 $Å^{-1}$). The component sums were normalized to 100 % (initial range: 74–129 %). Detailed information on each of the samples (sampled columns/locations, performed analyses) are given in Table 1.

| | | LCF-EXFAS results | | | | | | | | | | | R-factor[b] | Fe (%)[c] | S (%)[c] | Fe (%) bound to non-phyllosilicate phases[d] | S (%) bound to Jrs and/or Sch[e] |
|---|---|---|---|---|---|---|---|---|---|---|---|---|---|---|---|---|---|
| | | Primary silicate | | Secondary phyllosilicate | | Fe(II) phase | | Fe (hydr-)oxide | | | Fe oxyhydroxysulfate | | | | | | |
| | | Hbl[a] | Bt[a] | Chl | Ill | Aq. Fe(II) | Sd | 2-L Fh | Lep | Hem | Jrs | Sch | | | | | |
| Macropore surfaces | $R\text{-}1_{surf\text{-}2}$ | | | | 56 | | | | | | | 44 | 0.0379 | 6.08 | 0.59 | 2.65 | 0.19 |
| | $R\text{-}2_{surf\text{-}2}$ | 17 | | | 27 | | | | | | 16 | 39 | 0.0166 | 5.98 | 0.67 | 3.32 | 0.54 |
| | $R\text{-}2_{surf\text{-}3}$ | | | 19 | 28 | | | | | | 22 | 31 | 0.0685 | 7.14 | 1.07 | 3.82 | 0.76 |
| | $C_{2.5}\text{-}1_{surf}$ | | | | 56 | | | | 11 | | | 33 | 0.0263 | 7.90 | 0.52 | 1.17 | 0.19 |
| | $C_{2.5}\text{-}2_{surf}$ | | | 13 | 42 | | | | 10 | | | 34 | 0.0307 | 6.69 | 0.48 | 2.99 | 0.16 |
| | $C_{0.3}\text{-}1_{surf}$ | | | | 82 | | | | 18 | | | | 0.0816 | 5.24 | 0.13 | 0.92 | 0.00 |
| | $C_{0.3}\text{-}2_{surf}$ | 22 | | | 25 | | | 25 | | | | 28 | 0.0167 | 6.38 | 0.32 | 3.43 | 0.13 |
| | $P\text{-}1_{surf\text{-}2}$ | 23 | | | | | | | | | | 77 | 0.1535 | 5.78 | 0.23 | 4.43 | 0.32 |
| | $P\text{-}1_{surf\text{-}3}$ | | | | 81 | 19 | | | | | | | 0.2217 | 5.23 | 0.19 | 1.01 | 0.00 |
| | $P\text{-}2_{surf\text{-}2}$ | | | | 50 | | 13 | 24 | 13 | | | | 0.0325 | 5.86 | 0.23 | 2.96 | 0.00 |
| | $P\text{-}2_{surf\text{-}3}$ | 21 | | | 25 | | | | | | | 53 | 0.0280 | 6.94 | 0.33 | 3.71 | 0.26 |
| | $C_{2.5}P\text{-}1_{surf}$ | 19 | | | 17 | | | 25 | | | | 38 | 0.0141 | 7.88 | 0.32 | 5.01 | 0.21 |
| | $C_{2.5}P\text{-}2_{surf}$ | | 15 | | 24 | | | 33 | | | | 29 | 0.0086 | 8.10 | 0.30 | 4.97 | 0.17 |
| | $C_{0.3}P\text{-}1_{surf}$ | 17 | | | 26 | | | 23 | | | | 34 | 0.0148 | 6.96 | 0.43 | 3.92 | 0.17 |
| Interiors | $C_{2.5}\text{-}1_{int}$ | 39 | | | 36 | | | | | | | 25 | 0.0252 | 4.73 | 0.16 | 1.17 | 0.08 |
| | $C_{2.5}\text{-}2_{int}$ | 45 | | | 23 | | | | | | | 31 | 0.0604 | 4.08 | 0.17 | 1.28 | 0.09 |
| | $P\text{-}1_{int\text{-}2}$ | 47 | | | 40 | | | 13 | | | | | 0.0295 | 3.67 | 0.08 | 0.48 | 0.00 |
| | $P\text{-}1_{int\text{-}3}$ | 43 | | | 57 | | | | | | | | 0.0758 | 3.85 | 0.11 | 0.00 | 0.00 |
| | $P\text{-}2_{int\text{-}2}$ | 39 | | | 27 | | | 23 | | 11 | | | 0.0483 | 3.70 | 0.11 | 1.27 | 0.00 |
| | $P\text{-}2_{int\text{-}3}$ | 53 | | | 47 | | | | | | | | 0.1211 | 3.39 | 0.07 | 0.00 | 0.00 |
| | $C_{2.5}P\text{-}1_{int}$ | 33 | | | 31 | | | | | | | 35 | 0.0267 | 4.82 | 0.12 | 1.70 | 0.12 |
| | $C_{2.5}P\text{-}2_{int}$ | 34 | | | 26 | | | | | | | 40 | 0.0249 | 4.89 | 0.13 | 1.97 | 0.14 |

Hbl = Hornblende; Bt = Biotite; Chl = Chlorite; Ill = Illite; Aq.Fe(II) = Aqueous Fe(II); Sd = Siderite; 2-L Fh = 2-line ferrihydrite; Lep = Lepidocrocite; Hem = Hematite; Jrs = Jarosite; Sch = Schwertmannite.

[a] Due to the similarities in the EXAFS spectra of these two reference materials, the predicted fractional amounts for these minerals are uncertain.

[b] $R - factor = \Sigma((data - fit)^2 / \Sigma data^2)$

[c] Total concentrations of Fe or S determined by ICP-MS.

[d] Estimated by multiplying the sum of fitted proportions of non-phyllosilicate phases by the total concentrations of Fe.

[e] Estimated based on the fitted concentrations of Fe bound to schwertmannite (ideal formula, $Fe_8O_8(OH)_6SO_4$) and/or jarosite (ideal formula, $KFe_3(SO_4)_2(OH)_6$) as well as the ideal Fe/S molar ratios in these two Fe oxyhydroxysulfates.

of the Risöfladan field should have lower $O_2$ availability and thus could have contained more aqueous/labile Fe(II) and sulfide phases. These phases can be transported upwards by soil porewater or moisture through the macropore network (e.g., via evaporation driven capillary movement), continuously supplying them to well-aerated macropores in the oxidized horizon. Another source of these reduced species, as well as sulfate, is the interiors (within solid columnar blocks) that, as shown by (Högfors-Rönnholm et al., 2022), contain significant amounts of water-extractable Fe(II) (0.25–0.75 mg/kg). Following the supply of these species to the well-aerated macropores, either schwertmannite or jarosite could have been precipitated depending on the local physicochemical conditions (e.g., pH, levels of sulfate, and $K^+$, etc).

The accumulation of schwertmannite and jarosite on the macropore surfaces of the reference columns in terms of amounts (and to some extent also in terms of concentrations) led to a significant build-up of the $S_{NAS}$ fraction (approximately 8–9 g/kg, Fig. 2b), compared to the interiors whose $S_{NAS}$ concentrations were overall comparable with those reported for bulk acid sulfate soils in the tropical regions (Sukitprapanon et al., 2015; Yuan et al., 2015; Huang et al., 2016). The dissolution and hydrolysis of these iron oxyhydroxysulfates could not only result in a successive decrease in $S_{NAS}$, but also slow release of acidity and thus inhibit the recovery of soil pH. Previous studies have shown that the hydrolysis of jarosite is capable of buffering soil pH to approximately 3.5–4.0, even if the soil has been well-drained in the field or constantly flushed under experimental conditions (Mosley et al., 2017; Trueman et al., 2020). Similarly, the soils of this study have been drained for over 50 years in the field, followed by being constantly flushed with MQ for one month in our experiment. Despite that, the pH of the permeates from the two reference columns remained largely constant (close to 4), and Fe oxyhydroxysulfates as well as the $S_{NAS}$ fraction still occurred abundantly on the surfaces and in the interiors of the columns (Table 2; Figs. 1d,e, 2b). Thus, the oxidized horizons of the Risöfladan field and other similar acid sulfate soils are expected to continue discharging abundant acidic drainage and acting as a severe acidification hazard for a long time.

### *4.3. Transformations of iron oxyhydroxysulfates and associated loss of sulfate and retained acidity in treated soil columns*

In contrast to the reference columns, the columns treated with different mitigation suspensions did not contain any jarosite as predicted by the LCF-EXAFS analysis (Table 2). This is reasonable, because this mineral is only stable in highly-oxidizing (ORP > 400 mV) and acidic conditions (pH = 3–4), and will otherwise either not form or undergo dissolution and hydrolysis (Madden et al., 2012; Trueman et al., 2020; Kölbl et al., 2021). As reported by Högfors-Rönnholm et al. (2022), the treatments have led to a shift from oxic and acidic conditions in the reference columns to circumneutral/weakly-acidic and sub-oxic conditions in the treated soil columns. These treatment-induced conditions are outside the stability range of jarosite, thus favoring its dissolution and hydrolysis, in line with the absence of this mineral in all treated columns (Table 2). It has also been shown that chelating agents (e.g., organic ligands) could enhance the dissolution of jarosite either chemically or in combination with microbial activities (González et al., 2017; Tang et al., 2020; Trueman et al., 2020). Such processes might have facilitated the dissolution of jarosite in the peat-treated columns (P, $C_{2.5}P$, and $C_{0.3}P$), one of which (P) showed only a weak increase in pH (Högfors-Rönnholm et al., 2022). Sulfate released from dissolved jarosite can be quickly flushed out, giving a strong increase in sulfate concentrations in the permeates as observed by Högfors-Rönnholm et al. (2022) and shown here by the large S losses from all treated columns as compared to the reference columns (Figs. 1a, 2b).

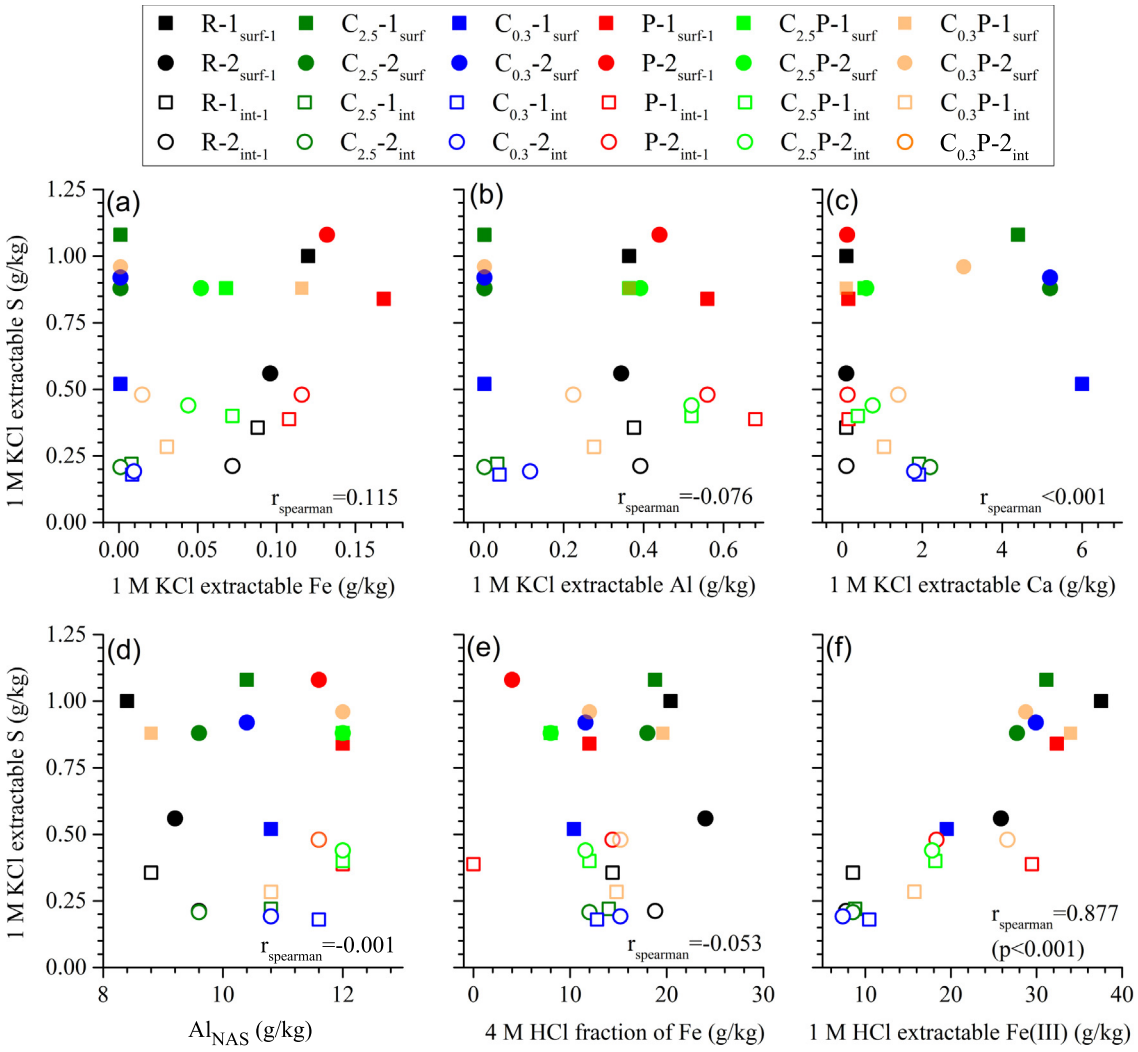


**Fig. 3.** The concentrations of 1 M KCl extractable S vs those of 1 M KCl extractable Fe (a), Al (b), and Ca (c) as well as $Al_{NAS}$ (d), 4 M HCl fraction of Fe (e), and 1 M HCl extractable Fe(III) (f). Detailed information on each of the samples (sampling columns/locations and performed analyses) are given in Table 1.

However, the released Fe(III) is expected to undergo a rapid hydrolysis process, forming nanoclusters of short-range order (SRO) iron hydroxides. These SRO iron hydroxides are unstable and can transform to more crystalline phases of higher thermodynamic stabilities such as lepidocrocite and goethite (Hansel et al., 2003; Pedersen et al., 2005). Indeed, lepidocrocite occurred and was the only Fe (hydr-)oxide in three out of four macropore-surface samples from the columns treated with pure calcite ($C_{2.5}$ and $C_{0.3}$), suggesting that SRO iron hydroxides formed via hydrolysis of Fe(III) from dissolving jarosite have been (near-)completely recrystallized. In contrast, the Fe (hydr-)oxide pools in the peat-treated columns were dominated by 2-line ferrihydrite, which is one of the most common SRO iron hydroxides in the surface environment. Given the well-documented inhibitory effect of organic matter on the recrystallization of SRO iron hydroxides (Eusterhues et al., 2008; Jones et al., 2009; Chen et al., 2015; Chen and Sparks, 2018), the persistence of 2-line ferrihydrite in the peat-treated columns was interpreted to reflect that peat-derived organic matter intimately reacted with (via surface absorption or aggregate occlusion) SRO iron hydroxides (structurally similar to 2-line ferrihydrite), effectively inhibiting their recrystallization processes over the time scales of our experiments.

Our LCF-EXAFS analysis revealed that schwertmannite occurred and was typically abundant on the macropore surfaces of all treated soil columns. This suggests that this mineral, in contrast to jarosite, was overall stable during all the treatments, that is, 3–4 weeks flushing with MQ or mitigation suspensions followed by 4-week incubation at 10 °C in dark). This is in accordance with the low reactivity of schwertmannite as observed for coastal lowland acid sulfate soils in Australia (Collins et al., 2010), as well as generally low transformation rates observed for (i) synthetic (and pure) schwertmannite incubated under acidic to near-neutral conditions in a chronically acidified natural acidic system (very limited transformation products were detected during the first 1–2 months) (Vithana et al., 2015); and (ii) natural schwertmannite (average transformation rate = 0.01–0.02 % $d^{-1}$) under controlled experimental conditions (25 °C, pH = 6 and 9) (Jönsson et al., 2005). The high amounts of schwertmannite in combination with the strong positive correlation between the 1 M HCl extractable Fe (III), expected to largely contain schwertmannite-bound Fe, and 1 M KCl extractable S (Fig. 3f) suggest that the liable S fraction was most likely derived from schwertmannite. Indeed, 1 M KCl can extract considerable amounts of sulfate from synthetic schwertmannite (Vithana et al., 2013). Schwertmannite can hold high proportions of outer-sphere complexed sulfate on its surface or within its tunnels (Wang et al., 2015), and these loosely-sorbed sulfate complexes can be easily released or exchanged with $OH^-$ under high pH conditions (Jönsson et al., 2005). Thus, the loosely-sorbed sulfate on schwertmannite can be released via an anion exchange reaction with $OH^-/CO_3^{2-}$ during the treatments with calcite ($C_{2.5}$, $C_{0.3}$, $C_{2.5}P$, and $C_{0.3}P$), contributing (in addition to jarosite dissolution) to the extensive increase in the discharge of sulfate from the calcite-treated columns, especially in the beginning of the treatments during

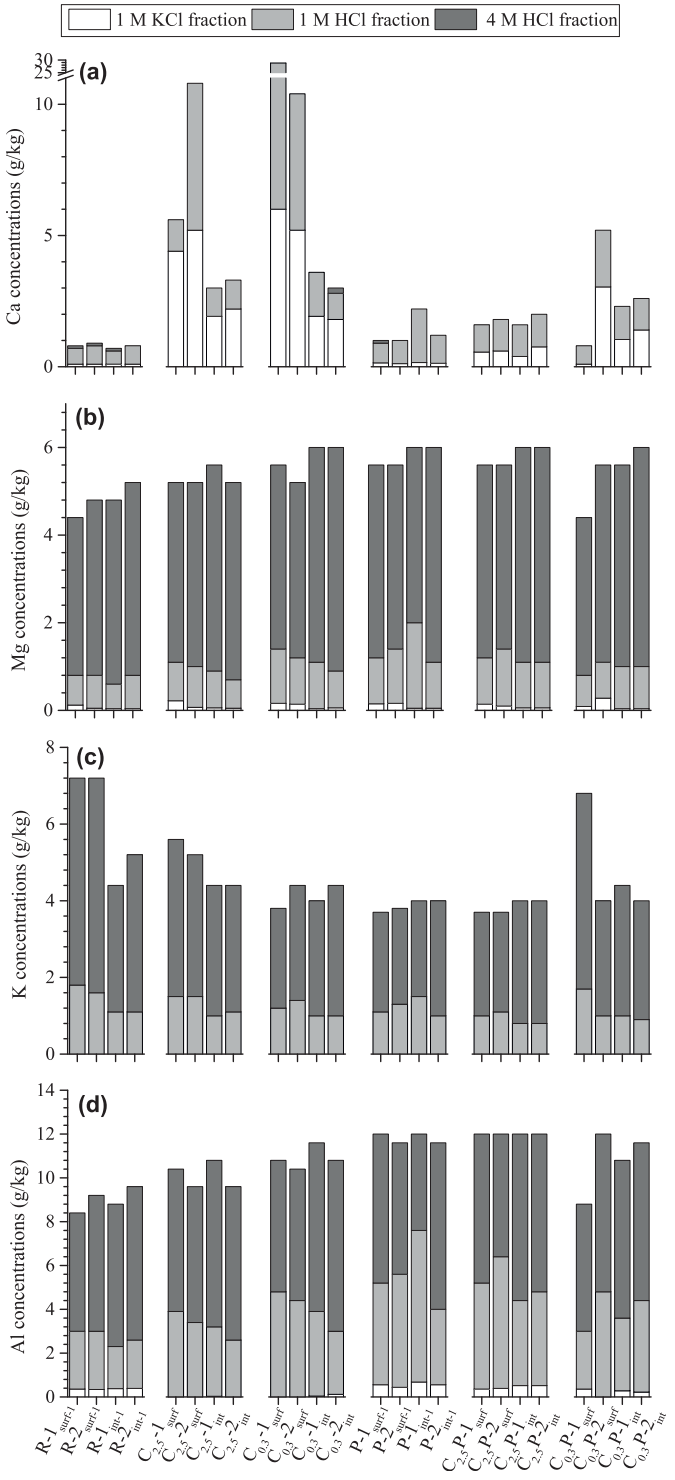


**Fig. 4.** Concentrations of different fractions of Ca, Mg, K, and Al on the macropore surfaces and in the interiors of the reference and treated soil columns. Detailed information on each of the samples (sampling columns/locations and performed analyses) are given in Table 1. The 4 M and 1 M HCl fractions were determined by difference: 4 M HCl extractable concentration – 1 M HCl extractable concentration and 1 M HCl extractable concentration – 1 M KCl extractable concentration, respectively.

which a dramatic increase in the release of sulfate was observed (Högfors-Rönnholm et al., 2022). Also, the columns treated with ultrafine-grained calcite ($C_{0.3}$ and $C_{0.3}$P) displayed a much more rapid and extensive release of sulfate than those treated with fine-grained calcite ($C_{2.5}$ and $C_{2.5}$P) (Högfors-Rönnholm et al., 2022), suggesting that calcite of smaller grain sizes are more effective in penetrating into macropores and reacting with the mineral phases on the macropore surfaces.

The columns treated only with peat (P1 and P2) displayed only a slight increase in pH (4.2–4.6) mirrored by a small decrease in ORP (263–427 mV), relative to the reference columns (pH = 4.1–4.2 and ORP = 440–480 mV) (Högfors-Rönnholm et al., 2022). These features indicated limited microbial reduction and linked proton-consuming processes during the peat treatment, which is further supported by the only minor amounts of secondary Fe(II) phases (e.g., aqueous $Fe^{2+}$ and siderite) on the macropore surfaces of these two columns (Table 2, Fig. 1b). For the columns treated with $C_{2.5}$ or $C_{0.3}$ in combination with P, the pH of the permeates remained around 6 during the treatment with P following the initial treatment with $C_{2.5}$ or $C_{0.3}$. Despite this pH being within the optimal range (pH = 5–8) for the growth of sulfate reducing bacteria (Neculita et al., 2007; Sanchez-Andrea et al., 2014), no Fe sulfide mineral was observed on the macropore surfaces of these columns (Table 2). The overall limited reduction of Fe and S during these treatments is in sharp contrast with greatly enhanced microbial reduction of Fe/S accompanied with marked changes in pH and ORP as observed for other acid sulfate soils amended with plant residues (e.g., wheat/pea straw, leaf/litter materials, plant shoots, etc) (Michael et al., 2015; Jayalath et al., 2016; Yuan et al., 2016; Kölbl et al., 2018) or their derived dissolved organic matter (Kölbl et al., 2022). In contrast to these plant residues, the peat materials used in our treatments have undergone a long-term degradation process in nature and thus, do obviously not contain sufficient easily-biodegradable organic molecules that are required to support high levels of microbial activity and biomass production in re-saturated acid sulfate soils (Kölbl et al., 2018). Thus, we ascribed the limited reduction of Fe(III) and sulfate in the peat-treated columns (P, $C_{2.5}$P, and $C_{0.3}$P) to low quality of the organic matter in the peat materials used for the treatments. However, the low levels of reduction (e.g., limited Fe(III) reduction and no/negligible sulfate reduction) and (near-)complete conversion of jarosite to Fe hydroxides observed for peat treatments are desirable, because (i) complete reduction of Fe and S will lead to the formation of Fe sulfides, which will be re-oxidized during future aeration events and ultimately result in renewed reacidification; and (ii) (near-)complete loss of jarosite (hosting most of the retained acidity in acid sulfate soils) will lead to a strong decrease in the acidity stored in the soils. Establishment of such weakly-moderately reducing conditions favoring the transformation of jarosite to Fe hydroxides while circumventing Fe-sulfide formation has been recently recommended as a desirable remediation option for jarosite-bearing sulfuric soils (Kölbl et al., 2021; Kölbl et al., 2022). In addition, as compared to the reference columns, the peat-treated columns released lower amounts of metals (e.g., Al, Co and Ni) (Högfors-Rönnholm et al., 2022), suggesting that peat can additionally act as efficient sorbents for metals under the weakly-acidic conditions.

## 5. Conclusions

This study investigated the geochemical status and processes of Fe and S on the surfaces of hydrologically active macropores and within solid columnar blocks ("interiors") of acid sulfate soil columns treated with MQ water (reference soil columns) and different mitigation suspensions (calcite, peat, and a successive combination of both). The main features and processes identified are:

- In natural state (reference columns), the surfaces of the macropores were, compared to the interiors, strongly enriched in Fe and S that were largely trapped as jarosite and schwertmannite (as distinct yellow-to-brownish coatings on the macropores).
- Slow dissolution and hydrolysis of Fe oxyhydroxysulfates (notably jarosite) on the macropore surfaces of the reference soil columns (representing typical acid sulfate soils in the boreal zone) released retained acidity and effectively buffered the soil at pH around 4. Thus, the Fe oxyhydroxysulfates accumulated on the macropore surfaces of boreal

acid sulfate soils are expected to act as long-term secondary acidification sources for the soils and nearby waterbodies.

- None of the treatments had a significant/notable effect on the stability of schwertmannite but led to a (near-)complete dissolution of jarosite accompanied by the formation of Fe hydroxides (mainly as lepidocrocite in soil columns treated only with calcite and as ferrihydrite in the others).
- The treatment with peat (presumably consisting mainly of well-decomposed organic matter) is a cheap and preferable remediation option. The organic-rich and weakly reductive condition created by this treatment favored the transformation of jarosite to Fe hydroxides but circumvented the formation of Fe sulfides, which would generate renewed acidification events upon re-oxidation.
- From all treated columns, S was extensively lost (leached) from both the macropore surfaces and interiors, explained by dissolution/transformation of jarosite and displacement of loosely-sorbed sulfate on schwertmannite. In contrast, Fe was not leached but retained as (hydr-) oxides in all treated columns.

## CRediT authorship contribution statement

**Changxun Yu:** Conceptualization, Methodology, Software, Formal analysis, Investigation, Writing – original draft, Writing – review & editing, Visualization. **Eva Högfors-Rönnholm:** Resources, Project administration, Writing – review & editing, Funding acquisition. **Pekka Sténn:** Writing – review & editing. **Sten Engblom:** Resources, Project administration, Writing – review & editing, Funding acquisition. **Mats E. Åström:** Conceptualization, Validation, Writing – review & editing, Funding acquisition.

## Data availability

Data will be made available on request.

## Declaration of competing interest

The authors declare that they have no known competing financial interests or personal relationships that could have appeared to influence the work reported in this paper.

## Acknowledgements

The study received funding from the Swedish Research Council Formas (contracts 2018-00760 to M.A. and 2020-01004 to C.Y.) and the European Regional Development Fund via the Interreg Botnia-Atlantica program to the project 'Sustainable treatment of coastal deposited sulfide soils (STASIS)'. The latter project received funding also from Region Västerbotten and Österbottens Förbund. Dr. Case M van Genuchten at the Geological Survey of Denmark and Greenland is thanked for helping collect Fe XAS data at the European Synchrotron Radiation Facility.

## Appendix A. Supplementary data

Supplementary data to this article can be found online at https://doi.org/10.1016/j.scitotenv.2022.159142.

## References

Ahern, C.R., McElnea, A., Sullivan, L., 2004. Acid Sulphate Soils: Laboratory Methods Guidelines. Department of Natural Resources, Mines and Energy.
Andriesse, W., Van Mensvoort, M., 2006. Acid sulfate soils: distribution and extent. Encyclopedia of Soil Science. 1, pp. 14–19.
Åström, M., 1998. Partitioning of transition metals in oxidised and reduced zones of sulphide-bearing fine-grained sediments. Appl. Geochem. 13 (5), 607–617.
Åström, M., Björklund, A., 1997. Geochemistry and acidity of sulphide-bearing postglacial sediments of western Finland. Environ. Geochem. Health 19 (4), 155–164.
Åström, M., Spiro, B., 2000. Impact of isostatic uplift and ditching of sulfidic sediments on the hydrochemistry of major and trace elements and sulfur isotope ratios in streams, Western Finland. Environ. Sci. Technol. 34, 1182–1188.
Åström, M., Österholm, P., Bärlund, I., Tattari, S., 2007. Hydrochemical effects of surface liming, controlled drainage and lime-filter drainage on boreal acid sulfate soils. Water Air Soil Pollut. 179 (1–4), 107–116.
Åström, M.E., Österholm, P., Gustafsson, J.P., Nystrand, M., Peltola, P., Nordmyr, L., Boman, A., 2012. Attenuation of rare earth elements in a boreal estuary. Geochim. Cosmochim. Acta 96, 105–119.
Bärlund, I., Tattari, S., Yli-Halla, M., 2005. Measured and simulated effects of sophisticated drainage techniques on groundwater level and runoff hydrochemistry in areas of boreal acid sulphate soils. Agric. Food Sci. 14 (1), 98–111.
Beven, K., Germann, P., 2013. Macropores and water flow in soils revisited. Water Resour. Res. 49 (6), 3071–3092.
Bigham, J., Nordstrom, D.K., 2000. Iron and aluminum hydroxysulfates from acid sulfate waters. Rev. Mineral. Geochem. 40 (1), 351–403.
Boman, A., Fröjdö, S., Backlund, K., Åström, M.E., 2010. Impact of isostatic land uplift and artificial drainage on oxidation of brackish-water sediments rich in metastable iron sulfide. Geochim. Cosmochim. Acta 74 (4), 1268–1281.
Burton, E.D., Johnston, S.G., 2012. Impact of silica on the reductive transformation of schwertmannite and the mobilization of arsenic. Geochim. Cosmochim. Acta 96, 134–153.
Burton, E.D., Bush, R.T., Sullivan, L.A., Mitchell, D.R.G., 2008. Schwertmannite transformation to goethite via the Fe(II) pathway: reaction rates and implications for iron–sulfide formation. Geochim. Cosmochim. Acta 72 (18), 4551–4564.
Canfield, D.E., 1988. Sulfate Reduction and the Diagenesis of Iron in Anoxic Marine Sediments. PhD thesis Yale University.
Chen, C., Sparks, D.L., 2018. Fe (II)-induced mineral transformation of ferrihydrite–organic matter adsorption and co-precipitation complexes in the absence and presence of as (III). ACS Earth Space Chem. 2 (11), 1095–1101.
Chen, C., Kukkadapu, R., Sparks, D.L., 2015. Influence of coprecipitated organic matter on Fe2+ (aq)-catalyzed transformation of ferrihydrite: implications for carbon dynamics. Environ. Sci. Technol. 49 (18), 10927–10936.
Claff, S.R., Sullivan, L.A., Burton, E.D., Bush, R.T., 2010. A sequential extraction procedure for acid sulfate soils: partitioning of iron. Geoderma 155 (3–4), 224–230.
Collins, R.N., Jones, A.M., Waite, T.D., 2010. Schwertmannite stability in acidified coastal environments. Geochim. Cosmochim. Acta 74 (2), 482–496.
Creeper, N.L., Hicks, W.S., Shand, P., Fitzpatrick, R.W., 2015a. Geochemical processes following freshwater reflooding of acidified inland acid sulfate soils: an in situ mesocosm experiment. Chem. Geol. 411, 200–214.
Creeper, N.L., Shand, P., Hicks, W., Fitzpatrick, R.W., 2015b. Porewater geochemistry of inland acid sulfate soils with sulfuric horizons following postdrought reflooding with freshwater. J. Environ. Qual. 44 (3), 989–1000.
Dang, T., Mosley, L.M., Fitzpatrick, R., Marschner, P., 2015. Organic materials differ in ability to remove protons, iron and aluminium from acid sulfate soil drainage water. Water Air Soil Pollut. 226 (11).
Dang, T., Mosley, L.M., Fitzpatrick, R., Marschner, P., 2016. Addition of organic material to sulfuric soil can reduce leaching of protons, iron and aluminium. Geoderma 271, 63–70.
Dent, D., 1986. Acid Sulphate Soils: A Baseline for Research and Development. ILRI.
Dent, D.L., Pons, L.J., 1995. A world perspective on acid sulphate soils. Geoderma 68 (3), 225.
Eusterhues, K., Wagner, F.E., Häusler, W., Hanzlik, M., Knicker, H., Totsche, K.U., Kögel-Knabner, I., Schwertmann, U., 2008. Characterization of ferrihydrite-soil organic matter coprecipitates by X-ray diffraction and Mossbauer spectroscopy. Environ. Sci. Technol. 42 (21), 7891–7897.
Fältmarsch, R.M., Åström, M.E., Vuori, K.M., 2008. Environmental risks of metals mobilised from acid sulphate soils in Finland: a literature review. Boreal Environ. Res. 13 (5), 444–456.
Favre, F., Jaunet, A., Pernes, M., Badraoui, M., Boivin, P., Tessier, D., 2004. Changes in clay organization due to structural iron reduction in a flooded vertisol. Clay Miner. 39 (2), 123–134.
Fitzpatrick, R.W., Mosley, L.M., Raven, M.D., Shand, P., 2017. Schwertmannite formation and properties in acidic drain environments following exposure and oxidation of acid sulfate soils in irrigation areas during extreme drought. Geoderma 308, 235–251.
Gill, R., 2014. Modern Analytical Geochemistry: An Introduction to Quantitative Chemical Analysis Techniques for Earth, Environmental and Materials Scientists. Routledge.
González, E., Muñoz, J.Á., Blázquez, M.L., González, F., Ballester, A., 2017. Reductive dissolution of jarosite by Acidiphilium cryptum in presence of chelating agents and dissolved iron. Geomicrobiol. J. 34 (4), 355–361.
Haese, R.R., Wallmann, K., Dahmke, A., Kretzmann, U., Müller, P.J., H.D., S., 1997. Iron species determination to investigate early diagenetic reactivity in marine sediments. Geochim. Cosmochim. Acta 61, 63–72.
Hall, G.E., 1998. Analytical perspective on trace element species of interest in exploration. J. Geochem. Explor. 63 (1–3), 1–19.
Hall, G., Vaive, J., Beer, R., Hoashi, M., 1996. Selective leaches revisited, with emphasis on the amorphous fe oxyhydroxide phase extraction. J. Geochem. Explor. 56 (1), 59–78.
Hansel, C.M., Benner, S.G., Neiss, J., Dohnalkova, A., Kukkadapu, R.K., Fendorf, S., 2003. Secondary mineralization pathways induced by dissimilatory iron reduction of ferrihydrite under advective flow. Geochim. Cosmochim. Acta 67 (16), 2977–2992.
Högfors-Rönnholm, E., Christel, S., Dalhem, K., Lillhonga, T., Engblom, S., Österholm, P., Dopson, M., 2018. Chemical and microbiological evaluation of novel chemical treatment methods for acid sulfate soils. Sci. Total Environ. 625, 39–49.
Högfors-Rönnholm, E., Sten, P., Stephan, C., Fröjdö, S., Lillhonga, T., Nowak, P., Österholm, P., Dopson, M., Engblom, S., 2022. Treatments targeting boreal acid sulfate soil hydrologically active macropore surfaces mitigate negative environmental effects. Appl. Geochem. Submitted for publication.
Huang, Q., Tang, S., Huang, X., Yang, S., Yi, Q., 2016. Characteristics of the acidity and sulphate fractions in acid sulphate soils and their relationship with rice yield. J. Agric. Sci. 154 (8), 1463–1473.
Hudd, R., Kjellman, J., 2002. Bad matching between hatching and acidification: a pitfall for the burbot, Lotalota, off the river Kyrönjoki,Baltic Sea. Fish. Res. 55 (1–3), 153–160.

Jarvis, N., 2007. A review of non-equilibrium water flow and solute transport in soil macropores: principles, controlling factors and consequences for water quality. Eur. J. Soil Sci. 58 (3), 523–546.
Jayalath, N., Mosley, L.M., Fitzpatrick, R.W., Marschner, P., 2016. Addition of organic matter influences pH changes in reduced and oxidised acid sulfate soils. Geoderma 262, 125–132.
Jayalath, N., Fitzpatrick, R., Mosley, L.M., Marschner, P., 2021. Addition of wheat straw to acid sulfate soils with different clay contents reduces acidification in two consecutive submerged-moist cycles. Geoderma 385.
Johnston, S.G., Bush, R.T., Sullivan, L.A., Burton, E.D., Smith, D., Martens, M.A., McElnea, A.E., Ahern, C.R., Powell, B., Stephens, L.P., Wilbraham, S.T., van Heel, S., 2009a. Changes in water quality following tidal inundation of coastal lowland acid sulfate soil landscapes. Estuar. Coast. Shelf Sci. 81 (2), 257–266.
Johnston, S.G., Hirst, P., Slavich, P.G., Bush, R.T., Aaso, T., 2009b. Saturated hydraulic conductivity of sulfuric horizons in coastal floodplain acid sulfate soils: variability and implications. Geoderma 151 (3–4), 387–394.
Jones, A.M., Collins, R.N., Rose, J., Waite, T.D., 2009. The effect of silica and natural organic matter on the Fe (II)-catalysed transformation and reactivity of Fe (III) minerals. Geochim. Cosmochim. Acta 73 (15), 4409–4422.
Jones, A.M., Collins, R.N., Waite, T.D., 2011. Mineral species control of aluminum solubility in sulfate-rich acidic waters. Geochim. Cosmochim. Acta 75 (4), 965–977.
Jönsson, J., Persson, P., Sjöberg, S., Lövgren, L., 2005. Schwertmannite precipitated from acid mine drainage: phase transformation, sulphate release and surface properties. Appl. Geochem. 20 (1), 179–191.
Karimian, N., Johnston, S.G., Burton, E.D., 2017. Antimony and arsenic behavior during Fe (II)-induced transformation of jarosite. Environ. Sci. Technol. 51 (8), 4259–4268.
Karimian, N., Johnston, S.G., Burton, E.D., 2018. Iron and sulfur cycling in acid sulfate soil wetlands under dynamic redox conditions: a review. Chemosphere 197, 803–816.
Kölbl, A., Marschner, P., Fitzpatrick, R., Mosley, L., Kögel-Knabner, I., 2017. Linking organic matter composition in acid sulfate soils to pH recovery after re-submerging. Geoderma 308, 350–362.
Kölbl, A., Marschner, P., Mosley, L., Fitzpatrick, R., Kögel-Knabner, I., 2018. Alteration of organic matter during remediation of acid sulfate soils. Geoderma 332, 121–134.
Kölbl, A., Kaiser, K., Winkler, P., Mosley, L., Fitzpatrick, R., Marschner, P., Wagner, F.E., Hausler, W., Mikutta, R., 2021. Transformation of jarosite during simulated remediation of a sandy sulfuric soil. Sci. Total Environ. 773, 145546.
Kölbl, A., Kaiser, K., Thompson, A., Mosley, L., Fitzpatrick, R., Marschner, P., Sauheitl, L., Mikutta, R., 2022. Rapid remediation of sandy sulfuric subsoils using straw-derived dissolved organic matter. Geoderma 420.
Ljung, K., Maley, F., Cook, A., Weinstein, P., 2009. Acid sulfate soils and human health—a millennium ecosystem assessment. Environ. Int. 35 (8), 1234–1242.
Madden, M.E., Madden, A., Rimstidt, J., Zahrai, S., Kendall, M., Miller, M., 2012. Jarosite dissolution rates and nanoscale mineralogy. Geochim. Cosmochim. Acta 91, 306–321.
Michael, P.S., Fitzpatrick, R., Reid, R., 2015. The role of organic matter in ameliorating acid sulfate soils with sulfuric horizons. Geoderma 255–256, 42–49.
Mosley, L.M., Biswas, T.K., Cook, F.J., Marschner, P., Palmer, D., Shand, P., Yuan, C., Fitzpatrick, R.W., 2017. Prolonged recovery of acid sulfate soils with sulfuric materials following severe drought: causes and implications. Geoderma 308, 312–320.
Muhrizal, S., Shamshuddin, J., Fauziah, I., Husni, M.A.H., 2006. Changes in iron-poor acid sulfate soil upon submergence. Geoderma 131 (1–2), 110–122.
Muhrizal, S., Shamshuddin, J., Husni, M.H.A., Fauziah, I., 2007. Alleviation of aluminum toxicity in an acid sulfate soil in Malaysia using organic materials. Commun. Soil Sci. Plant Anal. 34 (19–20), 2993–3011.
Neculita, C.M., Zagury, G.J., Bussiere, B., 2007. Passive treatment of acid mine drainage in bioreactors using sulfate-reducing bacteria: critical review and research needs. J. Environ. Qual. 36 (1), 1–16.
Nystrand, M.I., Österholm, P., Yu, C., Åström, M., 2016. Distribution and speciation of metals, phosphorus, sulfate and organic material in brackish estuary water affected by acid sulfate soils. Appl. Geochem. 66, 264–274.
Österholm, P., Åström, M., 2002. Spatial trends and losses of major and trace elements in agricultural acid sulphate soils distributed in the artificially drained Rintala area,W. Finland. Appl. Geochem. 17 (9), 1209–1218.
Österholm, P., Åström, M., Sundström, R., 2005. Assessment of aquatic pollution, remedial measures and juridical obligations of an acid sulphate soil area in western Finland. Agric. Food Sci. 14 (1), 44–56.
Österholm, P., Virtanen, S., Rosendahl, R., Uusi-Kämppä, J., Ylivainio, K., Yli-Halla, M., Mäensivu, M., Turtola, E., 2015. Groundwater management of acid sulfate soils using controlled drainage, by-pass flow prevention, and subsurface irrigation on a boreal farmland. Acta Agric. Scand. Sect. B Soil Plant Sci. 65 (sup1), 110–120.
Pedersen, H.D., Postma, D., Jakobsen, R., Larsen, O., 2005. Fast transformation of iron oxyhydroxides by the catalytic action of aqueous Fe (II). Geochim. Cosmochim. Acta 69 (16), 3967–3977.
Sanchez-Andrea, I., Sanz, J.L., Bijmans, M.F., Stams, A.J., 2014. Sulfate reduction at low pH to remediate acid mine drainage. J. Hazard. Mater. 269, 98–109.
Schoepfer, V.A., Burton, E.D., 2021. Schwertmannite: a review of its occurrence, formation, structure, stability and interactions with oxyanions. Earth Sci. Rev. 221.
Shahabi-Ghahfarokhi, S., Åström, M., Yu, C., Lindquisit, T., Djerf, H., Kalbitz, K., Ketzer, M., 2022. Extensive dispersion of metals from hemiboreal acid sulfate soil into adjacent drain and wetland. Appl. Geochem. 136.
Sukitprapanon, T., Suddhiprakarn, A., Kheoruenromne, I., Anusontpornperm, S., Gilkes, R., 2015. Forms of acidity in potential, active and post-active acid sulfate soils in Thailand. Thai J. Agric. Sci. 48 (3), 133–146.
Tang, Y., Xie, Y., Lu, G., Ye, H., Dang, Z., Wen, Z., Tao, X., Xie, C., Yi, X., 2020. Arsenic behavior during gallic acid-induced redox transformation of jarosite under acidic conditions. Chemosphere 255, 126938.
Trueman, A.M., McLaughlin, M.J., Mosley, L.M., Fitzpatrick, R.W., 2020. Composition and dissolution kinetics of jarosite-rich segregations extracted from an acid sulfate soil with sulfuric material. Chem. Geol. 543.
Vithana, C.L., Sullivan, L.A., Bush, R.T., Burton, E.D., 2013. Acidity fractions in acid sulfate soils and sediments: contributions of schwertmannite and jarosite. Soil Res. 51 (3), 203–214.
Vithana, C.L., Sullivan, L.A., Burton, E.D., Bush, R.T., 2015. Stability of schwertmannite and jarosite in an acidic landscape: prolonged field incubation. Geoderma 239–240, 47–57.
Wallmann, K., Hennies, K., König, I., Petersen, W., Knauth, H.-D., 1993. New procedure for determining reactive Fe (III) and Fe (II) minerals in sediments. Limnol. Oceanogr. 38 (8), 1803–1812.
Wang, X., Gu, C., Feng, X., Zhu, M., 2015. Sulfate local coordination environment in schwertmannite. Environ. Sci. Technol. 49 (17), 10440–10448.
Wang, S., Du, P., Yuan, P., Liu, Y., Song, H., Zhou, J., Deng, L., Liu, D., 2020. Structural alterations of synthetic allophane under acidic conditions: implications for understanding the acidification of allophanic andosols. Geoderma 376, 114561.
Wong, V.N.L., Johnston, S.G., Bush, R.T., Sullivan, L.A., Clay, C., Burton, E.D., Slavich, P.G., 2010. Spatial and temporal changes in estuarine water quality during a post-flood hypoxic event. Estuar. Coast. Shelf Sci. 87 (1), 73–82.
Wu, X., Wong, Z.L., Sten, P., Engblom, S., Osterholm, P., Dopson, M., 2013. Microbial community potentially responsible for acid and metal release from an Ostrobothnian acid sulfate soil. FEMS Microbiol. Ecol. 84 (3), 555–563.
Yli-Halla, M., Puustinen, M., Koskiaho, J., 2006. Area of cultivated acid sulfate soils in Finland. Soil Use Manag. 15 (1), 62–67.
Yu, C.X., Virtasalo, J.J., Karlsson, T., Peltola, P., Österholm, P., Burton, E.D., Arppe, L., Hogmalm, J.K., Ojala, A.E.K., Åström, M.E., 2015. Iron behavior in a northern estuary: large pools of non-sulfidized Fe(II) associated with organic matter. Chem. Geol. 413, 73–85.
Yu, C., Drake, H., Dideriksen, K., Tillberg, M., Song, Z., Morup, S., Astrom, M.E., 2020. A combined X-ray absorption and Mossbauer spectroscopy study on Fe valence and secondary mineralogy in granitoid fracture networks: implications for geological disposal of spent nuclear fuels. Environ. Sci. Technol. 54 (5), 2832–2843.
Yu, C., Xie, S., Song, Z., Xia, S., Åström, M.E., 2021. Biogeochemical cycling of iron (hydr-)oxides and its impact on organic carbon turnover in coastal wetlands: a global synthesis and perspective. Earth Sci. Rev. 218.
Yuan, C., Fitzpatrick, R., Mosley, L.M., Marschner, P., 2015. Sulfate reduction in sulfuric material after re-flooding: effectiveness of organic carbon addition and pH increase depends on soil properties. J. Hazard. Mater. 298, 138–145.
Yuan, C., Mosley, L.M., Fitzpatrick, R., Marschner, P., 2016. Organic matter addition can prevent acidification during oxidation of sandy hypersulfidic and hyposulfidic material: effect of application form, rate and C/N ratio. Geoderma 276, 26–32.